Magnetic-polarity stratigraphy of Siwalik Group sediments of Tinau Khola section in west central Nepal, revisited

Pitambar Gautam[1] and Erwin Appel[2]

[1]*Central Department of Geology, Tribhuvan University, Kirtipur, Kathmandu, Nepal*
[2]*Institut und Museum für Geologie und Paläontologie, Universität Tübingen, Sigwartstrasse* 10, D-72076 *Tübingen, Germany*

Accepted 1993 September 9. Received 1993 September 7; in original form 1993 June 25

SUMMARY

Remanent magnetization of sandstones sampled at 127 levels/sites throughout a 1710 m thick Siwaliks molasse sequence exposed along the Tinau Khola river in Nepal has been studied using thermal demagnetization. The magnetic remanence consists of: a secondary low-temperature component of normal polarity, unblocked mostly below 400–500 °C close to the present-day field, and a high-temperature characteristic remanence (ChRM) unblocked mostly between 600 and 685 °C, represented by both normal and reverse polarities. Demagnetization behaviour and isothermal remanence acquisition indicate that the secondary component resides on goethite and maghemite/magnetite whereas specular haematite carries ChRM. Anisotropy of magnetic susceptibility data reveals primary depositional magnetic fabric as judged by oblate ellipsoids and subvertical tilt-corrected minimum susceptibility axes.

A magnetic polarity sequence established using tilt-corrected ChRM directions from 124 levels reveals more details not found in the polarity stratigraphy worked out by Munthe *et al.* (1983). Comparison of the sequence with a standard polarity time-scale (Harland *et al.* 1989) suggests a depositional time range between *c.* 5.9 Ma (older than chron 3r) and 11 Ma (younger than chron 5r-2) for the section considered. According to new data, the horizon of *Sivapithecus punjabicus* falls close to the reversal boundary at *c.* 8.54 Ma (the lower age limit of the normal polarity chron 4Ar-1). Hence, the hominoid should be regarded as of *c.* 8.5 Ma rather than 9.0–9.5 Ma as suggested by Munthe *et al.* (1983).

Key words: Himalaya, magnetic polarity, magnetic susceptibility, magnetostratigraphy, remanent magnetization.

1 INTRODUCTION

The Miocene–Pleistocene fluvial molasse sediments of the Siwalik Group extending along the southern margin of the Himalayas possess a detailed record of the past geomagnetic polarity reversals and can be dated to a fine degree of resolution by using the technique of magnetostratigraphy, as shown by numerous studies in Pakistan and India (e.g. Opdyke *et al.* 1979; Tauxe & Opdyke 1982; Johnson *et al.* 1982, 1983; Flynn *et al.* 1990). In Nepal, the Siwalik Group comprises a ~6000 m thick coarsening-upward fluvial sequence of sediments deposited from 15 Ma to the Pleistocene and here too, during the last decade, magnetic polarity stratigraphy has been successfully applied in dating a number of sections: several sections in the Arung Khola–Binai Khola area (Tokuoka *et al.* 1986), the Surai Khola section (Appel, Rösler & Corvinus 1991) and the Bakiya Khola section (Harrison *et al.* 1993) (Fig. 1).

This study is concerned with the magnetic polarity stratigraphy of the Siwalik (Churia) Group sediments exposed along the Tinau Khola section in west central Nepal. Although magnetic polarity stratigraphy for this section was worked out by Munthe *et al.* (1983), which was the first attempt to use magnetostratigraphy to date the Siwalik sequence in Nepal, difficulty was found in using their '1800 m Lower Siwaliks' section and suggested polarity stratigraphy for detailed correlation with the recently mapped and magnetostratigraphically studied Siwaliks sections lying immediately towards east (Arung Khola–Binai Khola area) or west (Surai Khola area). So, it was decided to revisit the section but with a higher sampling density than before so as to get finer resolution. Sampling

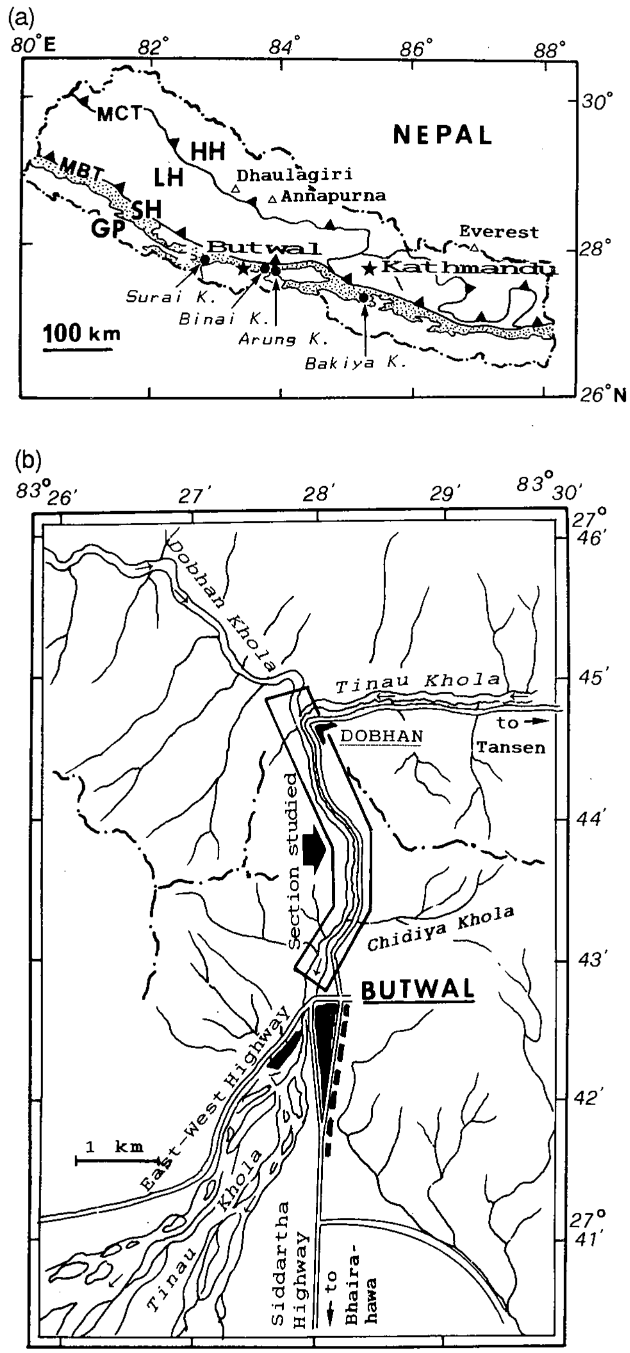

Figure 1. (a) Map of Nepal showing the distribution of the Siwalik Group (stippled). Major geographical divisions from north to south are: HH = Higher Himalaya; LH = Lesser Himalaya; SH = Sub-Himalaya; GP = Gangetic plain. MCT and MBT denote Main Central Thrust and Main Boundary Thrust, respectively. Tinau Khola section lies in the vicinity of the town, Butwal (27.71°N, 83.47°E). Localities of previous magnetostratigraphic studies in Nepalese Siwaliks (solid dots) are also indicated. (b) Map showing location of the Tinau Khola section studied, principal drainage systems and major highways around Butwal.

was confined to sandstones only because of their proven suitability in the Surai Khola section. Besides, the present study also aimed at establishing the nature of the magnetic fabric through the study of anisotropy of magnetic susceptibility.

2 BRIEF GEOLOGICAL OUTLINE

The Siwalik formations may represent, on a broad scale, temporally constrained depositional modes or asynchronous waves of different types of sediments that prograded into the Himalayan foredeep (Flynn *et al.* 1990). So even if lithological homogeneity exists over broad geographic areas, implying widespread similarity in the tectonic and/or climatic processes controlling depositional features, it does not indicate synchroneity of deposition. The time-transgressive nature of the boundary between Nagri and Dhok Pathan Formations firmly established in Siwaliks of Pakistan (*c.* 1 Myr: Barry, Beherensmeyer & Monaghan 1980) also proves these inferences. Consideration of the lateral variability of the lithofacies from area to area led Tokuoka *et al.* (1986) to refrain from the use of the well-known stratigraphic nomenclature of the Siwalik Group worked out in Pakistan, i.e. Lower Siwalik: Kamlial and Chinji; Middle Siwalik: Nagri and Dhok Pathan; and Upper Siwalik: Tatrot and Pinjore. Instead, based on detailed geological mapping of the Siwalik (Churia) Group rocks in between Arung Khola and Tinau Khola rivers, they suggested a fourfold lithostratigraphic division: Arung Khola Formation (A), Binai Khola Formation (B), Chitwan Formation (C) and Deorali Formation (D), in ascending order. In brief, the lithology (approximate thickness) of the formations in Arung Khola area is: (A) alternation of fine-grained sandstone and commonly variegated mudstone (2300 m); (B) thick-bedded, mainly medium to coarse grained, sometimes pebbly, sandstone with intercalation of non-variegated mudstone (2800 m): (C) gravel beds with subordinate sand and silt layers (700 m); and (D) unsorted angular to subangular boulder-conglomerate beds (450 m).

The present section along the Tinau Khola forms a part of the (Siwalik) Churia Group distributed in the southern belt (Tokuoka *et al.* 1990), whose southern margin is truncated by the Himalayan Frontal Thrust (HFT). The lowermost exposed section is represented by alternating beds of sandstone and occasionally variegated mudstones. The strata near the HFT are disturbed, show shallow to moderately steep NW dips and form the southern flank of an anticlinal structure. The oldest rocks are exposed at the axial part of an anticline, to the north of which all the strata show homoclinal northward dipping. The lithostratigraphic column shown in Fig. 2 starts just from the anticlinal axis.

All or most of the lower 790 m thickness of the section belongs to the upper member of the Arung Khola Formation. It consists of rhythmically alternating beds of quartzose, partly calcareous, normally up to 6–8 m thick sandstone, and usually up to 4–6 m thick, sometimes variegated mudstone. Sandstones tend to gradually coarsen upsection giving a pepper-and-salt appearance and also thicken, individual beds reaching up to 15–20 m in thickness, in the same direction. Several mudstone beds yield molluscan fossils and well-preserved plant leaves (levels indicated as F8903, F65 and F66). The uppermost part has yielded *Sivapithecus* (*Ramapithecus*) *punjabicus*, as reported by Munthe *et al.* (1983).

A 200 m thick sequence, which consists of alternations of

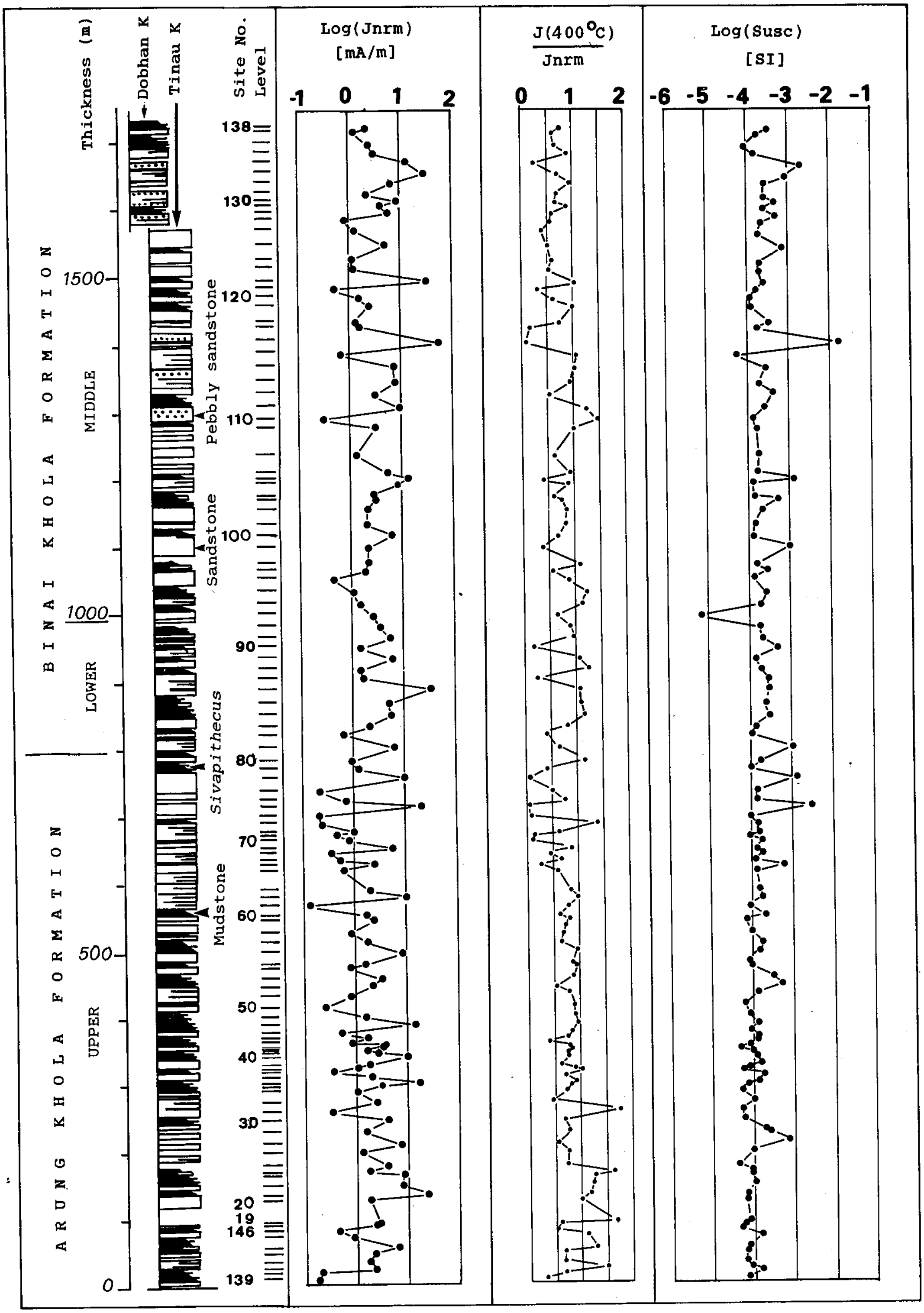

Figure 2. Simplified lithologic column, sampling levels and selected rock magnetic properties throughout the studied section. Log(Jnrm): logarithm of natural remanent magnetization intensity; J(400 °C)/Jnrm: ratio of residual remanence intensity at 400° C to the natural remanent magnetization intensity; Susc: susceptibility. The position of the horizon yielding *Sivapithecus punjabicus* (Munthe *et al.* 1983) is also indicated.

thick-bedded pepper-and-salt type sandstone, fine-grained sandstone and mudstone, the last of these yielding plant remains, represents the lower member of the Binai Khola Formation (Bl).

The 720 + m sequence following upward is related to the middle member of the Binai Khola Formation (Bm). It is composed of thick-bedded, massive, pepper-and-salt sandstones intercalated with thin mudstones. Pebble conglomerates are sometimes intercalated with the sandstones. Basal, granule-bearing sequences of the thick-bedded sandstones contain mammal bones. The thickness of sandstone beds is typically several metres but may reach 25–30 m. Trough and planar cross laminations are well developed, and channel and scouring structures with rip-up clasts are common.

3 SAMPLING AND LABORATORY PROCEDURE

One to three sandstone core samples, 2.54 cm in diameter and 4–12 cm in length, were obtained from 146 sites/levels using a portable gasoline-powered drill engine and oriented with a magnetic compass. 18 sites (T1–T18) in the lowermost part represent a structurally disturbed SW-dipping section some 120 m thick, and as such represent the repeated basal part of the continuous section represented by 128 sites (T139–T146 and T19–T138). The 1710 m thick section (Figs 1 and 2) considered starts actually at the axial part of the anticline exposed in the right bank of Tinau Khola, some 350 m downstream from the confluence with Chidiya Khola, is continuous, undeformed and has 18°–62° northwards dips. Mean sampling density is 13.4 m of the thickness of the section.

Several standard specimens of 2.2–2.5 cm length were cut from these samples in the laboratory for measurement of the remanence and magnetic susceptibility. A variety of instruments was employed: a LETI RS 01 cryogenic magnetometer for measurement of remanence of at least one specimen from each level; shielded TSD-1 (Schonstedt) or MMTD1 (Magnetic Measurements) furnaces for progressive thermal demagnetization; kappabridge KLY-2 (Geofyzika Brno) for measuring low-field susceptibility after each heating step in order to monitor heating-induced mineral alterations as well as for determining the anisotropy of susceptibility; an electromagnet capable of producing magnetic fields up to 1.5 T to impart IRM; a fluxgate spinner magnetometer (Digico) to measure the isothermal remanence produced after each step of magnetization acquisition; and an induction spinner magnetometer JR-5 (Geofyzika Brno) for remanence measurements of additional 37 thermally demagnetized specimens plus 16 IRM-treated specimens. Measurements were carried out using the facilities available at the palaeomagnetic laboratories of the Institute of Geophysics, Munich University, and Institute of Geology and Palaeontology, Tübingen University, Germany.

4 MAGNETIC REMANENCE, MAGNETO-MINERALOGY AND ANISOTROPY OF MAGNETIC SUSCEPTIBILITY

NRM intensity for 127 specimens ranged between 0.13 and 54 mA m^{-1} (mean: 4.4 mA m^{-1}) and usually remained well above the noise levels (about 0.01 mA m^{-1} for LETI RS 01 and 0.0024 mA m^{-1} for JR-5) of the magnetometers after thermal demagnetization at 400–500 °C. The ratio of the intensity remained after 400 °C demagnetization to the initial NRM intensity, i.e. $J(400\,°C)/J(\mathrm{NRM})$ ranges from 0.04 to 1.75 and has a mean of 0.76. Intensity ratios exceeding 1.0 are confined exclusively to those specimens in which a normal polarity component (subparallel to the present-day field direction) superimposed over a high unblocking temperature remanence of reverse polarity (with declination nearly antiparallel to that of the present-day field direction) became demagnetized during the initial steps of thermal demagnetization. In the majority of specimens, only a quarter of the total remanent magnetization is due to thermally less stable components. Very low intensity ratios, on the other hand, are observed in relatively coarse-grained specimens. Susceptibility for most specimens is around 10^{-4} SI but varies widely between 5.9×10^{-6} and 14.6×10^{-3} SI, i.e. by a factor of 2500. The lithologic column and the variation of NRM intensity, susceptibility and intensity ratio with stratigraphic height is shown in Fig. 2. In general, the logarithmic susceptibility magnitudes tend to increase linearly with the stratigraphic height. This probably results from a gradual increase in the contribution of ferrimagnetic minerals (probably magnetite and maghemite) towards upper levels in this generally coarsening-upward sequence.

At least one specimen per site was subjected to step-wise thermal demagnetization in progressively higher temperature steps, which ranged from six to ten from room temperature to 675 °C. Demagnetization trajectories for specimens viewed in orthogonal vector end-point diagrams (Fig. 3a) are: (1) essentially linear, i.e. no directional change during demagnetization (specimen T22B); (2) having two discrete linear segments indicating the presence of components of differing unblocking temperature spectra (specimen T133); (3) having one or more linear segments followed by irregular changes in directions without clear-cut convergence to the origin (specimens T118B); and (4) curvilinear without any clear linear segments (specimen T61). Fig. 3(b) shows the changes in direction and intensity of the NRM of these specimens during demagnetization. Specimens from 82 levels showed type (1) or (2) trajectories and the ChRM from each specimen was isolated by principal component analysis (PCA: Kirschvink 1980) and designated as class A directions. To test the consistency of the measurement, one or two sister specimens from the remaining levels in which the first batch of specimens exhibited type (3) and (4) trajectories, were additionally demagnetized using 10 heating steps. Specimens from 22 levels exhibited the presence of a high blocking temperature direction revealed generally only between 600 and 675 °C such that three or more data points lying on linear segment were not available and so PCA could not be applied. In such cases, directions at a single temperature step or averages of directions at two or more temperature steps from one or more specimens from the same level were determined to get the estimates of ChRM and designated as class B directions. Demagnetization data from 20 specimens, which did not show stable end-points but had great circle trends in the equal-area projections (e.g. specimens T61 and T118B, Fig. 3b), were subjected to remagnetization circle analysis using the procedure outlined by McFadden & McElhinny (1988). This procedure gave the estimates of expected ChRM, categorized as class C directions. Specimens from three levels (sites T76, T96 and T112), all represented by medium to coarse sandstones showed irregular uninterpretable changes in directions upon demagnetization and no directional information could be extracted from site T64 because of loss of orientation mark.

Acquisition of IRM and its thermal demagnetization response for specimens representative of the collection is shown in Fig. 4. Specular haematite is present in all

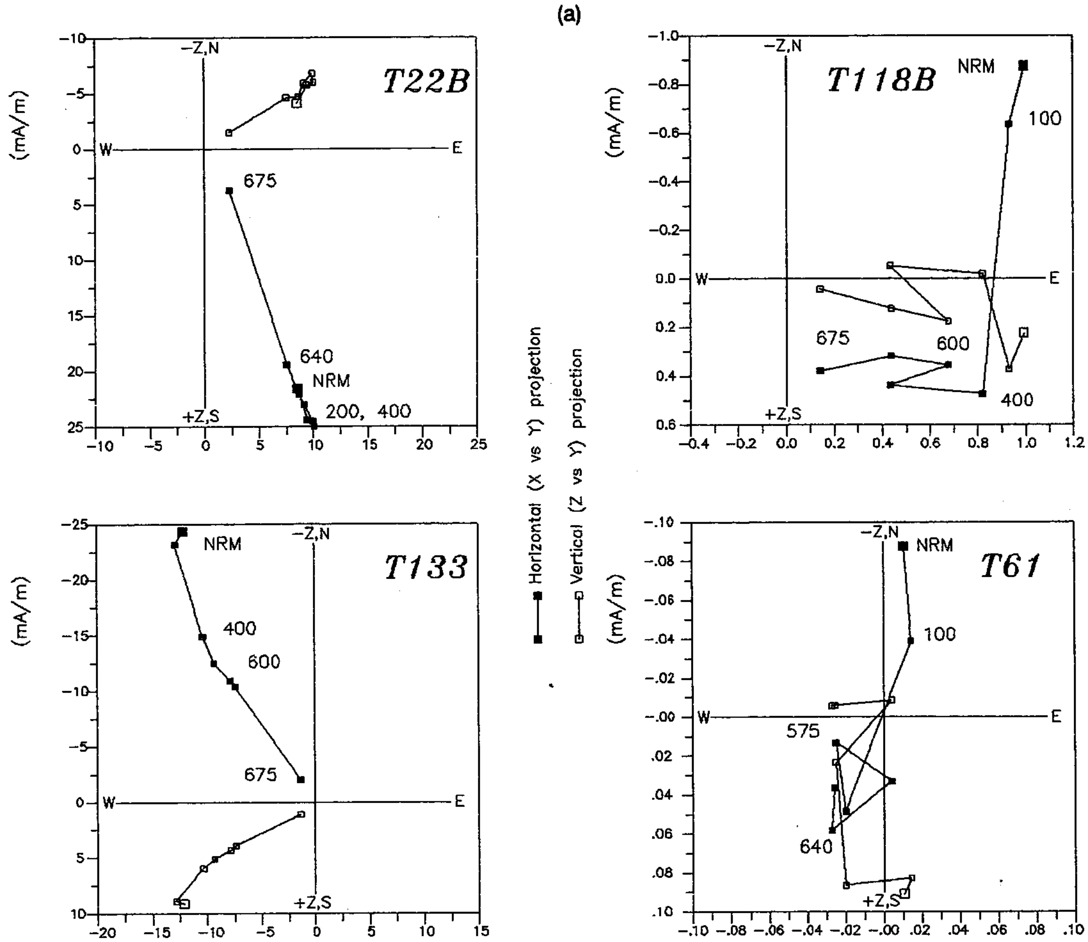

Figure 3(a). Orthogonal vector plots showing demagnetization behaviour of representative specimens (T22B, T133, T61 and T118B) upon thermal demagnetization. Numbers besides the projection points indicate peak demagnetization temperatures (°C). Directions are corrected for bedding.

specimens because a part of the remanence is unblocked above 600 °C and always continues up to its Curie point. Samples rich in haematite have moderate IRM (200 mT)/IRM (1500 mT) ratios, generally in the range 0.6–0.8, and a large fraction of remanence remains above 600 °C (e.g. T22A). Magnetite/maghemite-rich specimens have an IRM ratio between 0.8 and 1.0 because of early saturation in low fields and very high saturation intensity (e.g. T113). Presence of goethite in significant amounts can be easily recognized by a sharp decay of the remanence below 100 °C and a very low IRM ratio (<0.35; e.g. T119A). Amounts of maghemite are believed to be significant, especially in medium-grained sandstones (e.g. T61).

Anisotropy of magnetic susceptibility was determined in sandstone specimens from 112 levels (Gautam & Pant 1993, and in preparation). The apparent lack of correlation between the NRM intensities and magnitudes of susceptibility (Fig. 2) probably results from: (1) the contribution of ferrimagnetic as well as paramagnetic particles to the magnetic susceptibility; and (2) the multicomponent nature of the remanence, in particular, the superposition of normal polarity soft component over nearly antipodal reverse polarity ChRM in about half of the collections. Mean values for the shape factor E (Hrouda 1982) and P factor (Nagata 1961) are 1.04 ± 0.04 and 1.06 ± 0.06, respectively. The degree of anisotropy, defined as h per cent $= 100 \times (k_1 - k_3)/(k_1 + k_2 + k_3)$, where k_i, $i = 1, 2, 3$, denote the maximum, intermediate and minimum eigenvalues of the susceptibility tensor, is <6 per cent for all but three specimens with a mean around 2 per cent. The data suggest oblate ellipsoids, subvertical tilt-corrected minimum susceptibility axes and subhorizontal magnetic foliation almost parallel to the bedding plane. The magnetic fabric thus seems to be primary and did not undergo any significant post-depositional disturbances. It implies that the ChRM is of primary depositional origin (Tauxe *et al.* 1990).

5 SUMMARY OF REMANENCE DIRECTIONS

Specimens from 97 levels showed the presence of reasonably linear (mean angular deviation < 15°) segments below 400–500 °C and the line fitting yielded directions with northerly declinations and moderately steep downward inclinations. The directions, in geographic coordinates, cluster around the present-day dipole field direction ($I = 47°$) and yield a mean with the following statistics

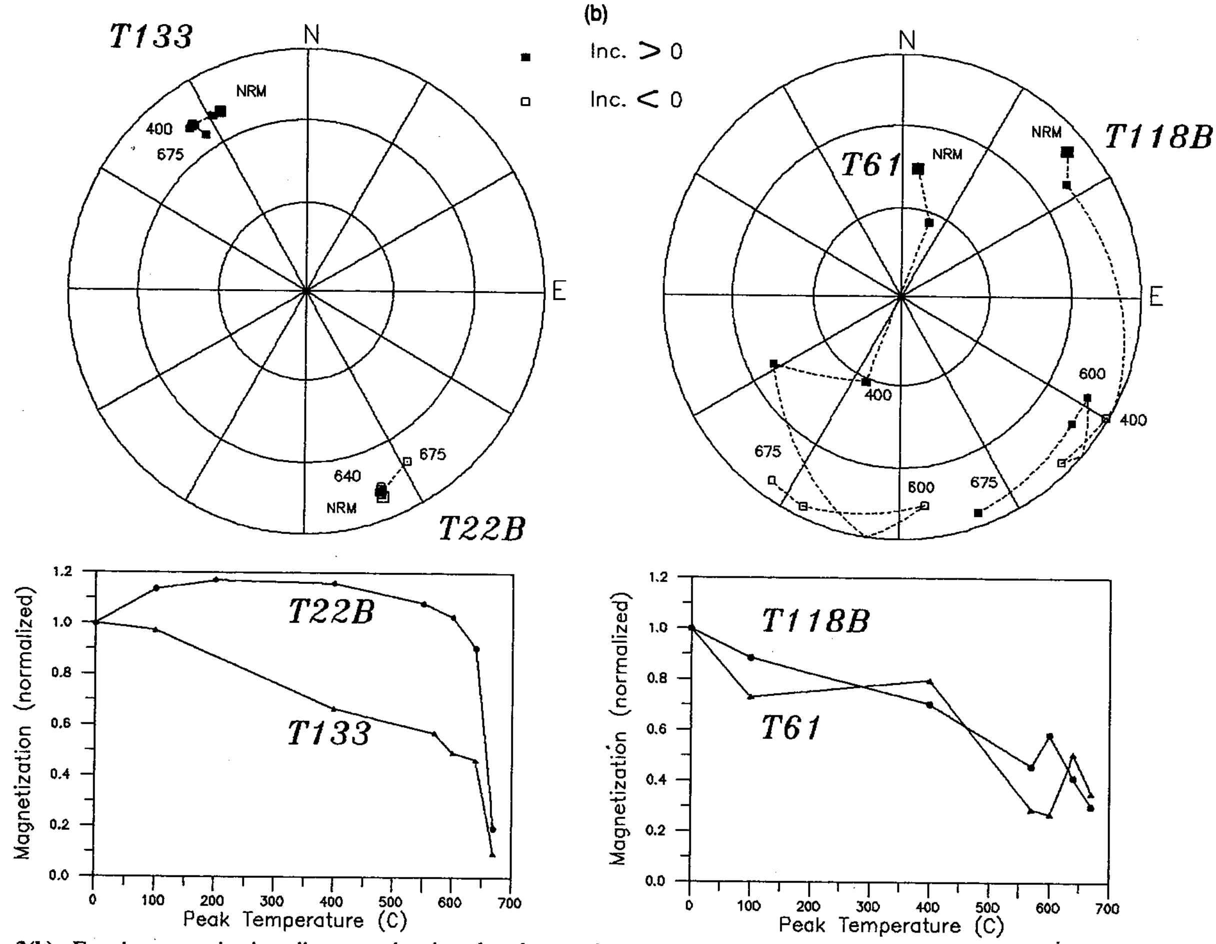

Figure 3(b). Equal-area projection diagrams showing the changes in resultant magnetization vectors during thermal demagnetization and intensity response curves for specimens mentioned in Fig. 3(a). Directions are corrected for bedding.

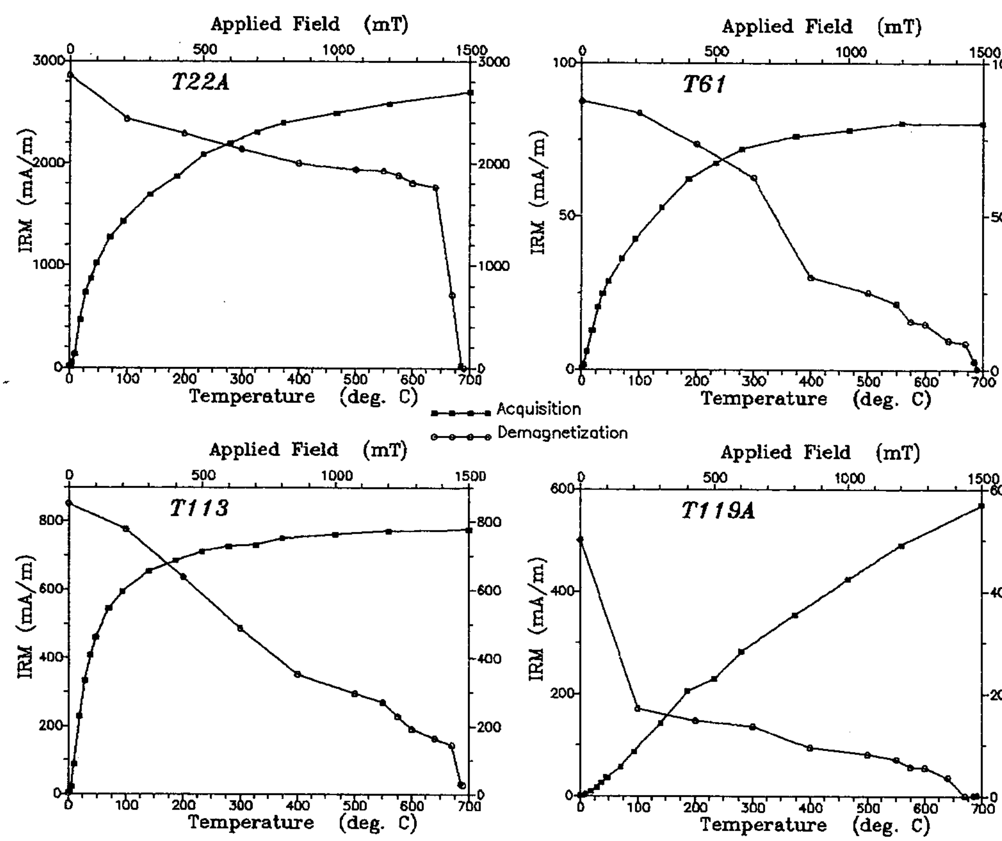

Figure 4. Curves showing acquisition of isothermal remanent magnetization (IRM) and behaviour during demagnetization of IRM for representative specimens.

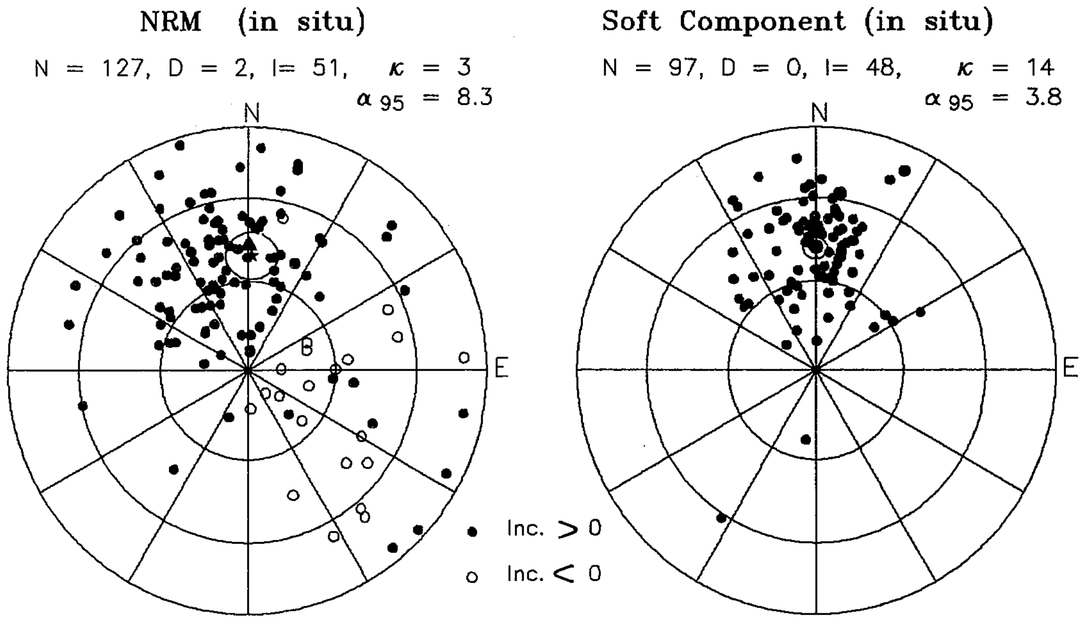

Figure 5. Equal-area projections of *in situ* NRM directions of specimens from all levels and *in situ* soft-component directions (least-squares line fitting of three or more points; MAD < 15°) obtained from specimens at 97 levels. Mean directions (stars) and associated confidence ellipses are also shown. Triangle in the left diagram stands for dipole field direction ($I = 47°$) at Butwal.

(Fisher 1953): $N = 97$, $D = 0°$, $I = 48°$, $k = 13.9$, $\alpha_{95} = 3.8°$. Clearly, this is a secondary viscous remanence carried by magnetite/maghemite or haematite, or a chemical remanence carried by goethite. Owing to the presence of this component there is obvious clustering of initial NRM directions around the present-day field direction (Fig. 5).

Tilt-corrected ChRM directions (classes A, B and C; mentioned above) from 124 levels fall into two antipodal regions indicating dual polarity nature (Fig. 6a). Polarity assignment could in principle be based on declinations (northerly–normal; southerly–reverse) but calculated VGP latitudes (moderately positive–normal; moderately negative–reverse) were easier to use. Polarity at 121 levels could be easily determined using VGP values and occasionally declinations as well (Fig. 7). For levels T87, T97 and T103, for which the declinations estimates obtained are either easterly or westerly, VGP values were not decisive. Polarity in these levels was determined taking into

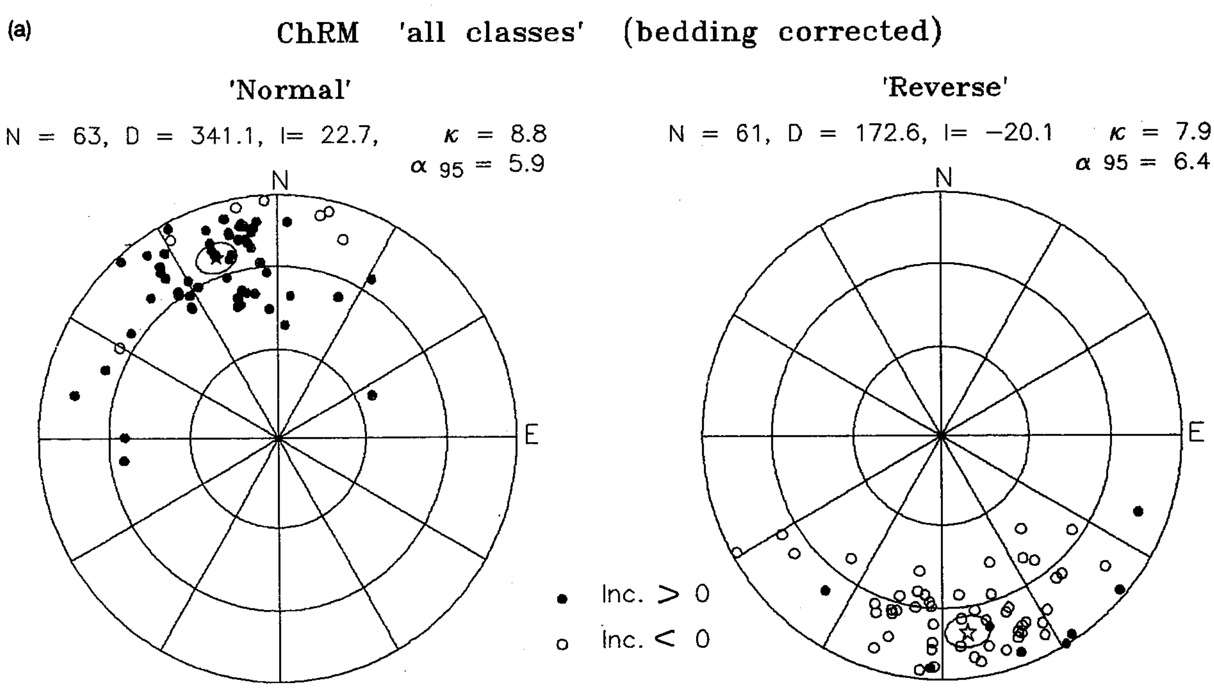

Figure 6(a). Equal-area projections of bedding-corrected characteristic remanence (ChRM) directions comprising all classes (A, B and C).

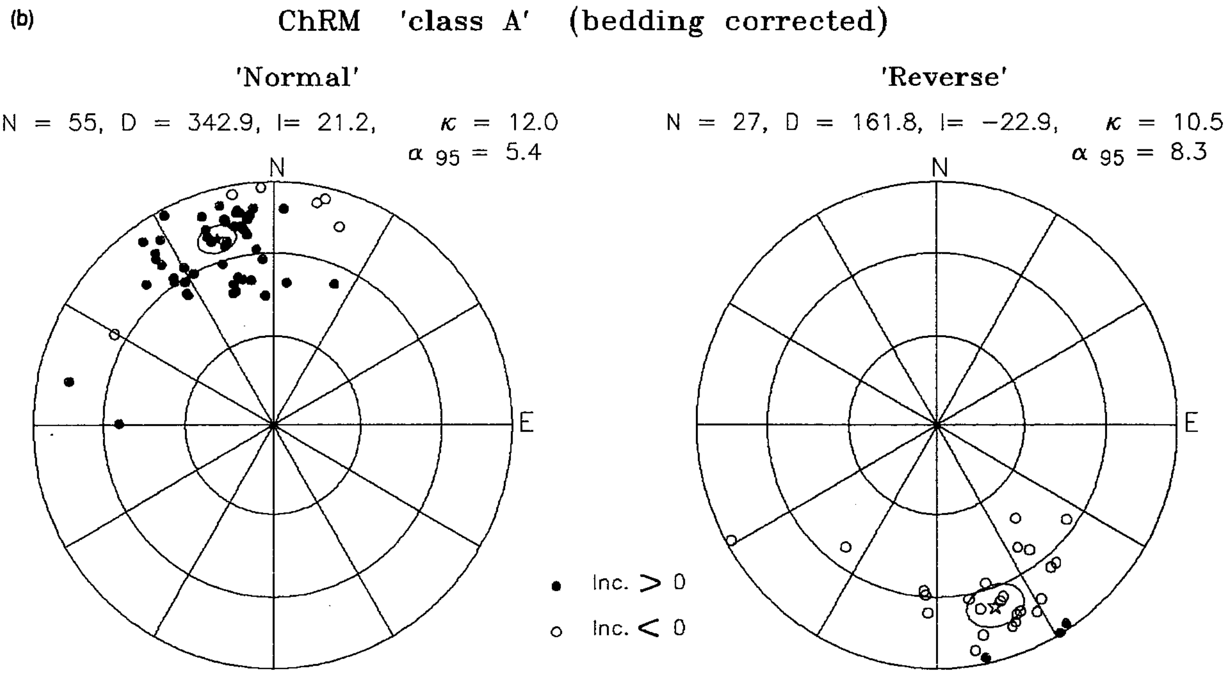

Figure 6(b). Equal-area projections of bedding-corrected 'class A' ChRM directions.

account the inclination values and also the demagnetization behaviour of multiple specimens. Directions from all levels yield following mean for each polarities:

Normal: $N = 63$, $D = 341.1°$, $I = 22.7°$, $k = 8.8$, $\alpha_{95} = 5.9°$.
Reverse: $N = 61$, $D = 172.6°$, $I = -20.1°$, $k = 7.9$, $\alpha_{95} = 6.4°$.

If only class A directions are taken into consideration, we get the following mean values:

Normal: $N = 55$, $D = 342.9°$, $I = 21.2°$, $k = 12.0$, $\alpha_{95} = 5.4°$.
Reverse: $N = 27$, $D = 161.8°$, $I = -22.9°$, $k = 10.5$, $\alpha_{95} = 8.3°$.

These directions are shown in Fig. 6(b). It is obvious that the ChRM passes the reversal test. The mean inclination of 22°, based on class A data, is interpreted as a combined effect of: (1) inclination shallowing due to haematite grains, and (2) the acquisition of the remanence at latitudes shallower than the present-day location owing to the northward drift of the Indian Plate since the Miocene. The averaged expected inclination for the study area during 11–6 Ma (the age range for the section studied estimated in this study; see Section 6) after taking into account an average rate of northward drift of the Indian plate as 5 cm yr^{-1} (e.g. Patriat & Achache 1984) would be around 42°. Hence, the observed inclination is shallower by 20° than the expected inclination and the ratio of tangents of the observed and expected inclinations is about 0.45. These observations are consistent with findings reported by numerous field and also experimental studies on Siwalik Group sediments (e.g. Tauxe & Opdyke 1982; Tauxe & Kent 1984; Johnson *et al.* 1983; Appel *et al.* 1991). There is a significant declination anomaly (20° westward relative to the present-day declination; 16–18° westward relative to the expected direction during 11–6 Ma) and it suggests the presence of a counter-clockwise rotation of the Tinau Khola section. Such rotation, however, is most probably of a local nature because no such significant discrepancy was found in the Surai Khola section (Appel *et al.* 1991).

6 MAGNETIC-POLARITY STRATIGRAPHY, SEDIMENT ACCUMULATION RATES AND IMPLICATIONS TO THE AGE OF THE HOMINOID

Directions obtained from specimens at 124 levels have been used to establish the magnetic-polarity sequence (MPS) (Fig. 7). Individual polarity reversals are recognized even if supported by a single specimen, because either the direction comes from a least-squares line fit (class A) or the directional consistency among specimens from the same level has been firmly established using one or two sister specimens (class B and class C). In order to assign the age to the MPS, we use the standard polarity time-scale of Harland *et al.* (1989). The long interval of predominantly normal polarity observed between 167 m and 614 m is correlated with chron 5n. Further correlation is based on matching reversal patterns. The correlation seems straightforward through the entire section except for the interval 1247 m to 1492 m. The studied section is found to range between chron 5r-2 and middle of chron 3A with corresponding age between *c.* 11 Ma and 5.9 Ma spanning over 5 Myr (Fig. 8). The polarity stratigraphy proposed by Munthe *et al.* (1983) is also shown in Fig. 8 to facilitate the comparison. The present MPS reveals more details not seen in the previous polarity stratigraphy. We believe that the lack of details in previous polarity stratigraphy could be due to the low number of sampling sites ($N = 63$) and, more so, due to the

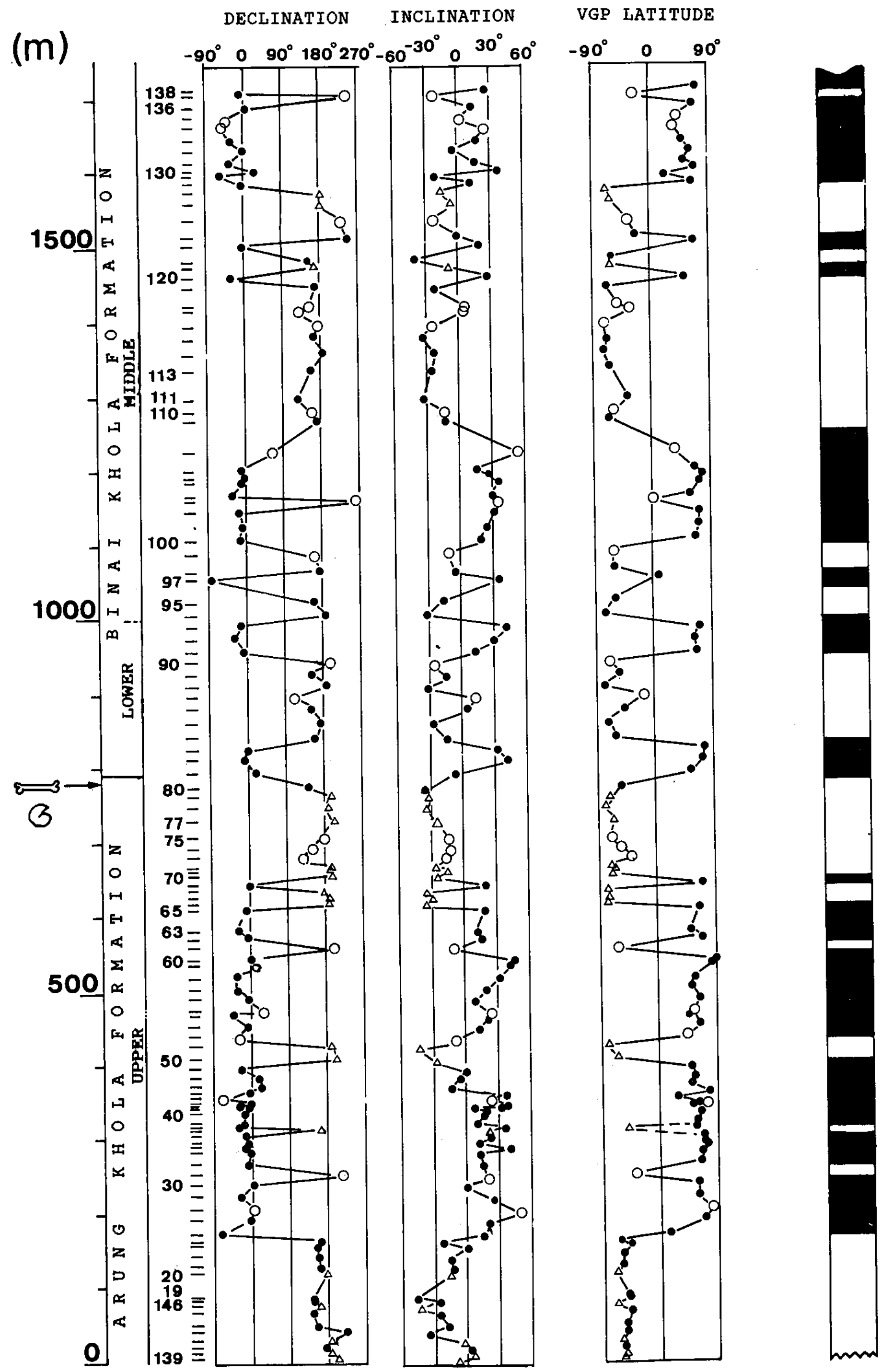

Figure 7. Declinations, inclinations and VGP latitudes plotted against the thickness and the inferred magnetic polarity sequence. Dots, circles and triangles represent class A, class B and class C data, respectively. Black and white intervals in the polarity sequence represent normal and reverse polarities, respectively.

inadequateness of the blanket-alternating field demagnetization to remove the haematite- and goethite-based secondary remanence (Appel *et al.* 1991).

Relative changes in sedimentation rate and its quantitative estimate are shown in Fig. 9. Each bar shows the sedimentation rate based on the stratigraphic thickness of a particular well-defined polarity interval and the time range obtained through correlation with the standard time-scale. The rate for the entire section varies from about 11 to 83 cm kyr^{-1} with an average of 34 cm kyr^{-1}. Three episodes of relatively fast sediment deposition roughly corresponding to 8.8–8.3 Ma, 7.7–7.5 Ma and 7.2–6.7 Ma may be recognized. Relatively high sedimentation rates, much higher than the average 20–50 cm kyr^{-1}, were also

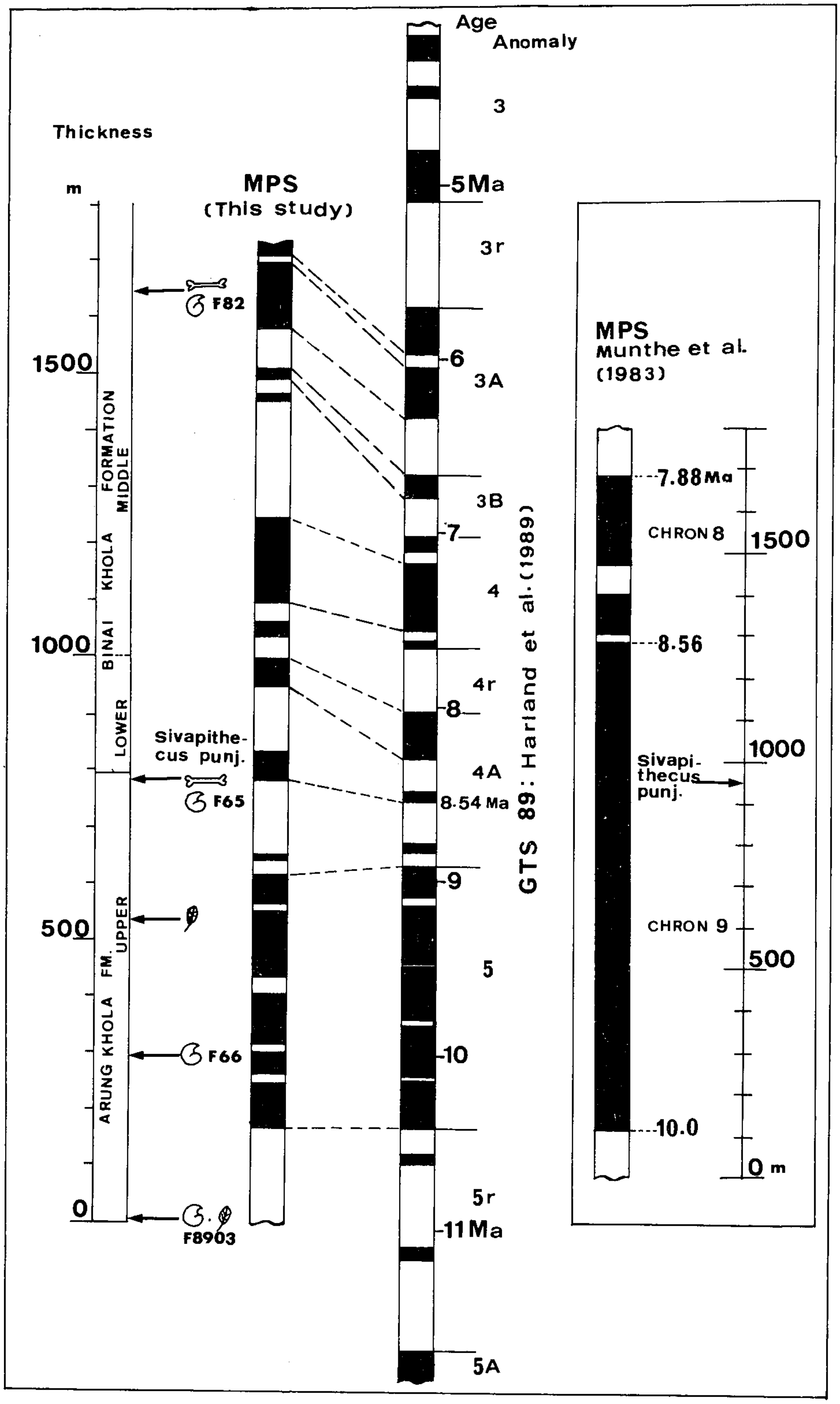

Figure 8. Correlation of the Tinau Khola magnetic polarity sequence (MPS) with the standard polarity time-scale of Harland *et al.* (1989). The MPS after Munthe *et al.* (1983) is shown on the right for reference. Black: normal polarity; white: reverse polarity.

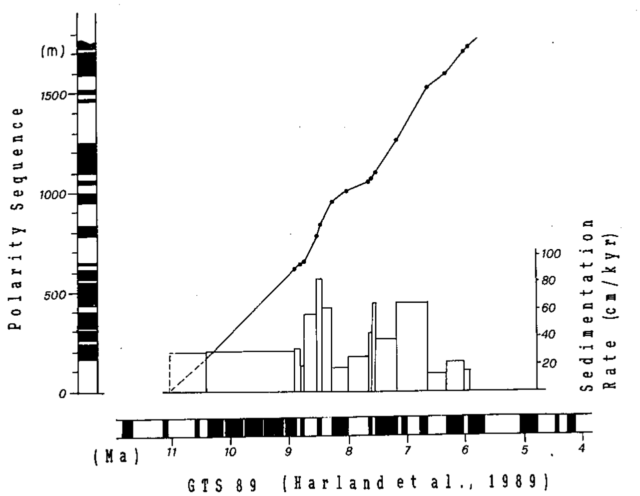

Figure 9. Sedimentation rates for the Tinau Khola section deduced from the polarity sequence plotted versus a standard polarity time-scale. The slope of the deduced curve varying with time (Ma) is directly proportional to the sedimentation rate. The bar diagram shows the average sedimentation rates for specific time periods.

suggested for the Binai Khola lower member from the Arung Khola area (Tokuoka *et al.* 1986) and similar highs characterize the Surai Khola and Bakiya Khola sections around 9 Ma and 6.5–7 Ma (Appel *et al.* 1991; Harrison *et al.* 1993). So, not only the range but also the elevated magnitudes of the sedimentation rate derived in this study seem to be consistent with the observations throughout the studied Siwaliks section in Nepal. The three periods of rapid deposition in the Tinau Khola Siwaliks correspond to the deposition of sand-dominated (650–950 m and 1040–1100 m) and pebbly- to sand-dominated (1250–1525 m) sections (Figs 2, 8 and 9). In these sections, the sandstones have a generally pepper-and-salt appearance and they are very rich in biotite served from the schistose, granitic and gneissose rocks in the Higher Himalayas which presumably experienced rapid upheaval (Tokuoka *et al.* 1986) during the deposition of these sandstones. It will be worthwhile to note that recent studies (Amano and Taira 1992) on the sedimentation pattern and the provenance of the sediments deposited in the distal Bengal fan suggest 'an acme of uplift' of the Higher Himalayas between 10.9 and 7.5 Ma.

Details revealed in the present MPS have implications to the age of the hominoid. The horizon yielding *Sivapithecus punjabicus* (Munthe *et al.* 1983) falls very close to the lower boundary of chron 4Ar-1 (8.54 Ma) and thus can be dated at *c.* 8.5 Ma. This new age is younger by 0.5–1.0 Myr than the 9.0–9.5 Myr old age suggested by Munthe *et al.* (1983).

Flynn *et al.* (1990) note that large remains of the *Sivapithecus* recovered from 42 Y-GSP localities in Potwar Siwaliks, Pakistan, belong to 22 independent levels while 13 other sites are known from various sources. The time span that contains the local origination and extinction of *Sivapithecus* with 95 per cent confidence is 13.5–6.4 Ma using 22 levels, or 13.1–6.8 Ma while using 35 levels. Extinction of *Sivapithecus* at around 7 Ma is suggested by Johnson *et al.* (1983) from Haritalyangar (India). Further, it has been suggested (Flynn *et al.* 1990) that the disappearance age of the arboreal, forest-adapted ape is related to the sudden change of dominantly C3 (forest plant) community to C4 (grassland) community observed at around 7 Ma. More precisely, such change took place at 7.4 Ma in Potwar Siwaliks, 7.0 Ma in Bakiya Khola and 6.6 Ma in Surai Khola, based on the stable carbon ratio in palaeosols and pedogenic carbonates (Quade, Cerling & Bowman 1989; Harrison *et al.* 1993; Cater *et al.* 1993). As the Tinau Khola is concerned, Tanaka (1992) has observed an ecological shift from C3-dominated to C4-dominated biomass conditions to take place during the depositional time of the upper member of Arung Khola Formation and the lower member of the Binai Khola Formation. The 8.5 Myr old age for the *Sivapithecus* suggested in this study falls within the age range that was dominated by forest plant community.

ACKNOWLEDGMENTS

We thank S. R. Pant and S. Tanaka for their help and discussions during the field work. We also appreciate the help of M. Weiß, W. Rösler and A. Patzelt at various stages of laboratory work. We gratefully acknowledge the comments of Lisa Tauxe and another anonymous reviewer to improve the manuscript. This research is an outcome of a collaborative research programme between the Tribhuvan University, Nepal and University of Tubingen, Germany. We acknowledge the financial support given by the German Research Council (DFG).

REFERENCES

Amano, K. & Taira, A., 1992. Two-phase uplift of Higher Himalayas since 17 Ma, *Geology,* **20,** 391–394.

Appel, E., Rösler, W. & Corvinus, G., 1991. Magnetostratigraphy of the Miocene–Pleistocene Surai Khola Siwaliks in West Nepal, *Geophys. J. Int.,* **105,** 191–198.

Barry, J.C., Beherensmeyer, A.K. & Monaghan, M., 1980. A geologic and biostratigraphic framework for Miocene sediments near Khaur village, northern Pakistan, *Postilla,* **183,** 1–19.

Cater, J.M.L., Quade, J., Schelling, D.D., Jones, M.A., Seago, R.D. & Opdyke, N.D., 1993. Late Miocene climatic and tectonic events during the deposition of the Siwalik Group in southern Nepal, *J. Geol.,* in press.

Fisher, R.A., 1953. Dispersion on a sphere, *Proc. R. Soc. Lond.,* **217,** 295–305.

Flynn, L.J., Pilbeam, D., Jacobs, L.L., Barry, J.C., Behrensmeyer, A.K. & Kappelman, J.W., 1990. The Siwaliks of Pakistan: time and faunas in a Miocene terrestrail setting, *J. Geol.,* **98,** 589–604.

Gautam, P. & Pant, S.R., 1993. Anisotropy of magnetic susceptibility of the Tinau Khola Siwaliks sediments, West Central Nepal, in *Abstracts, Seminar on Himalayan Geology & Geophysics,* Wadia Inst. Him. Geol., Dehradun, India.

Harland, W.B., Armstrong, R.L., Cox, A.V., Craig, L.E., Smith, A.G. & Smith, D.G., 1989. The magnetostratigraphic time scale, in *A Geologic Time Scale,* pp. 140–167, Cambridge University Press, Cambridge.

Harrison, T.M., Copeland, P., Hall, S.A., Quade, J., Burner, S., Ojha, T.P. & Kidd, W.S.F., 1993. Isotopic preservation of Himalayan/Tibetan uplift, denudation, and climatic histories in two molasse deposits, *J. Geol.,* **101,** 157–175.

Hrouda, F., 1982. Magnetic anisotropy of rocks and its application in geology and geophysics, *Geophys. Surv.,* **5,** 37–82.

Johnson, N.M., Opdyke, N.D., Johnson, G.D., Lindsay, E.H. & Tahirkheli, R.A.K., 1982. Magnetic polarity stratigraphy and ages of Siwalik Group rocks of the Potwar Plateau, Pakistan, *Paleogeog. Paleoclimat. Paleoecol.*, **37,** 17–42.

Johnson, G.D., Opdyke, N.D., Tandon, S.K. & Nanda, A.C., 1983. The magnetic polarity stratigraphy of the Siwalik group at Haritalyangar (India) and a new last appearance datum for Ramapithecus and Sivapithecus in Asia, *Palaeogeog. Palaeoclimat. Palaeoecol.*, **44,** 223–249.

Kirschvink, J.L., 1980. The least-squares line and plane and the analysis of palaeomagnetic data, *Geophys. J.R. astr. Soc.*, **62,** 699–718.

McFadden, P.L. & McElhinny, M.W., 1988. The combined analysis of remagnetization circles and direct observations in palaeomagnetism, *Earth planet. Sci. Lett.*, **87,** 161–172.

Munthe, J., Dongol, B., Hutchison, J.H., Kean, W.F., Munthe, K. & West, R.M., 1983. New fossil discoveries from the Miocene of Nepal include a hominoid, *Nature,* **303,** 331–333.

Nagata, T., 1961. *Rockmagnetism,* Maruzen, Tokyo.

Opdyke, N.D., Lindsay, E., Johnson, G.D., Johnson, N.M., Tahirkheli, R.A.K. & Mirza, M.A., 1979. Magnetic polarity stratigraphy and vertebrate paleontology of the Upper Siwalik subgroups of Northern Pakistan, *Paleogeog. Paleoclimat. Paleoecol.*, **27,** 1–34.

Patriat, P. & Achache, J., 1984. India–Eurasia collision chronology has implications for crustal shortening and driving mechanism of plates, *Nature,* **311,** 615–621.

Quade, J., Cerling, T.E. & Bowman, J.R., 1989. Dramatic ecologic shift in the latest Miocene of northern Pakistan, and its significance to the development of the Asian Monsoon, *Nature,* **342,** 163–166.

Tanaka, S., 1992. Paleosols from Middle Miocene–Pleistocene in the Churia (Siwalik) Group, West Central Nepal, in *Abstracts, Symposium on Himalayan Geology,* Shimane 92, Japan.

Tauxe, L. & Kent, D.V., 1984. Properties of a detrital remanence carried by haematite from study of modern river deposits and laboratory redeposition experiments, *Geophys. J. R. astr. Soc.*, **77,** 543–561.

Tauxe, L. & Opdyke, N.D., 1982. A time framework based on magnetostratigraphy for Siwalik sediments of the Khaur area, northern Pakistan, *Paleogeog. Paleoclimat. Paleoecol.*, **37,** 43–61.

Tauxe, L., Constable, C., Stokking, L. & Badgley, C., 1990. Use of anisotropy to determine the origin of characteristic remanence in the Siwalik red beds of Northern Pakistan, *J. geophys. Res.*, **95** (B4), 4391–4404.

Tokuoka, T., Takayasu, K., Hisatomi, K., Yamasaki, H., Tanaka, S., Konomatsu, M., Sah, R.B. & Rai, S.M., 1990. Stratigraphy and geologic structures of the Churia (Siwalik) Group in the Tinau Khola–Binai Khola area, West Central Nepal, *Mem. Fac. Sci., Shimane Univ.*, **24,** 71–88.

Tokuoka, T., Takayasau, K., Yoshida, M. & Hisatomi, K., 1986. The Churia (Siwalik) Group of the Arung Khola area, West Central Nepal, *Mem. Fac. Sci., Shimane Univ.*, **20,** 135–210.